EBioMedicine 3 (2016) 141–154

Contents lists available at ScienceDirect

EBioMedicine

journal homepage: www.ebiomedicine.com

Research Paper

Hypothermic Preconditioning Reverses Tau Ontogenesis in Human Cortical Neurons and is Mimicked by Protein Phosphatase 2A Inhibition

Nina M. Rzechorzek [a,b,c,*], Peter Connick [d,1], Matthew R. Livesey [c,e,1], Shyamanga Borooah [b,c,d], Rickie Patani [d,f], Karen Burr [b,c], David Story [b,c], David J.A. Wyllie [c,e], Giles E. Hardingham [e], Siddharthan Chandran [a,b,c,d,*]

[a] Centre for Clinical Brain Sciences, University of Edinburgh, Edinburgh, Midlothian EH16 4SB, United Kingdom
[b] MRC Centre for Regenerative Medicine, University of Edinburgh, Edinburgh, Midlothian EH16 4UU, United Kingdom
[c] Euan MacDonald Centre for MND Research, University of Edinburgh, Edinburgh, Midlothian EH16 4SB, United Kingdom
[d] The Anne Rowling Regenerative Neurology Clinic, University of Edinburgh, Edinburgh, Midlothian EH16 4SB, United Kingdom
[e] Centre for Integrative Physiology, University of Edinburgh, Edinburgh, Midlothian EH8 9XD, United Kingdom
[f] Department of Molecular Neuroscience, UCL Institute of Neurology, Queen Square, London WC1N 3BG, United Kingdom

ARTICLE INFO

Article history:
Received 7 August 2015
Received in revised form 10 December 2015
Accepted 11 December 2015
Available online 12 December 2015

Keywords:
Hypothermia
Preconditioning
Neuroprotection
Tau protein
Protein phosphatase 2A (PP2A)
Hyperphosphorylation
Human cortical neuron

ABSTRACT

Hypothermia is potently neuroprotective, but the molecular basis of this effect remains obscure. Changes in neuronal tau protein are of interest, since tau becomes hyperphosphorylated in injury-resistant, hypothermic brains. Noting inter-species differences in tau isoforms, we have used functional cortical neurons differentiated from human pluripotent stem cells (hCNs) to interrogate tau modulation during hypothermic preconditioning at clinically-relevant temperatures. Key tau developmental transitions (phosphorylation status and splicing shift) are recapitulated during hCN differentiation and subsequently reversed by mild (32 °C) to moderate (28 °C) cooling — conditions which reduce oxidative and excitotoxic stress-mediated injury in hCNs. Blocking a major tau kinase decreases hCN tau phosphorylation and abrogates hypothermic neuroprotection, whilst inhibition of protein phosphatase 2A mimics cooling-induced tau hyperphosphorylation and protects normothermic hCNs from oxidative stress. These findings indicate a possible role for phospho-tau in hypothermic preconditioning, and suggest that cooling drives human tau towards an earlier ontogenic phenotype whilst increasing neuronal resilience to common neurotoxic insults. This work provides a critical step forward in understanding how we might exploit the neuroprotective benefits of cooling without cooling patients.

1. Introduction

The lack of neuroprotective treatments for acute and chronic brain disorders presents a major challenge to modern medicine. Therapeutic hypothermia is a rare example of a proven neuroprotective intervention — however, it is only practically useful in restricted patient groups (Yenari and Han, 2012; Jacobs et al., 2013; Andrews et al., 2015). Improved mechanistic understanding of neuroprotective hypothermia could reveal novel molecular targets with which to exploit the protective effect of cooling in a wider clinical context. Against this background, a range of experimental systems and studies of hibernating animals have implicated several pathways that might mediate hypothermic neuroprotection (Arendt et al., 2003; Chip et al., 2011; Yenari and Han, 2012; Rzechorzek et al., 2015). A potentially important candidate is microtubule-associated protein tau. Specifically, reversible hyperphosphorylation of tau in hibernating, hypothermic and developing brains – brains which are comparatively resistant to injury – suggests cold-inducible changes in tau might contribute to hypothermic neuroprotection (Mawal-Dewan et al., 1994; Arendt et al., 2003; Planel et al., 2007; Stieler et al., 2011).

Interspecies differences in cellular and molecular biology have impeded translation of neuroprotective strategies from pre-clinical models to man. With regard to tau, a potentially significant species difference lies in the developmentally-regulated expression of its multiple isoforms (Janke et al., 1999). The relative abundance of tau isoforms determines tau function in health and disease (Trojanowski and Lee, 1995), therefore this balance might be altered under conditions that influence neuronal survival, such as hypothermia. Whilst there is little evidence of this effect in in vivo models of hypothermic neuroprotection (Stieler et al., 2011), several core human tau isoforms are absent in the adult rodent brain (Janke et al., 1999). These observations provide a strong

* Corresponding authors at: Centre for Clinical Brain Sciences, University of Edinburgh, Edinburgh, Midlothian EH16 4SB, United Kingdom.
E-mail addresses: nina.rzechorzek@ed.ac.uk (N.M. Rzechorzek), siddharthan.chandran@ed.ac.uk (S. Chandran).
[1] These authors contributed equally to this work.

http://dx.doi.org/10.1016/j.ebiom.2015.12.010

rationale to explore tau in the context of hypothermic neuroprotection in a physiologically relevant human system.

We recently established an experimental platform of functional hCNs (Bilican et al., 2014; Livesey et al., 2014) and demonstrated its value for exploring molecular mechanisms of hypothermic preconditioning (Rzechorzek et al., 2015). Here we show that hCN differentiation recapitulates the principal features of early human cortical tau development which are subsequently reversed by hypothermia, returning tau transcriptionally and post-translationally to an earlier ontogenic state. Further we confirm that cooling protects these neurons in an injury- and temperature-specific manner (Rzechorzek et al., 2015). Finally we provide evidence that cooling-induced hCN tau hyperphosphorylation results from a disproportionate suppression of protein phosphatase 2A (PP2A) relative to glycogen synthase kinase 3β (GSK3β) (Planel et al., 2007), which is both necessary and sufficient to protect hCNs from oxidative stress. These findings establish a role for PP2A inhibition in hypothermic preconditioning of human neurons and suggest that phospho-tau may participate in this neuroprotective effect.

2. Materials and Methods

2.1. Differentiation of hCNs

hCNs were differentiated from expanded anterior neural precursors (aNPCs) as described elsewhere (Bilican et al., 2014; Livesey et al., 2014; see also Supplemental Materials and Methods). Briefly, upon removal of FGF2, aNPCs (passages 17 to 39) were plated in 12 or 24-well plates (Nunc) at 1×10^5 cells cm^{-2} onto glass coverslips coated with Poly-L-Ornithine (1 in 1000, Sigma), Laminin (1 in 100, Sigma), Fibronectin (10 μg/ml, Sigma) and Reduced growth-factor Matrigel® (1 in 200, BD Biosciences). Differentiating aNPCs were cultured in default media at 3% O_2, 5% CO_2, 37 °C. For KCl stimulation experiments aNPCs were differentiated in Matrigel® (1 in 100)-coated 6-well plates at the same density. Cultures were fed twice weekly until 21 d, after which they were fed every other day. Periodic testing with a PCR-based detection kit (Minerva Biolabs) confirmed that both precursor and differentiated cultures were *Mycoplasma*-free. For developmental characterization, samples were harvested at aNPC stage and 14, 28, 42 and 49 d after plating for differentiation. Electrophysiological characterization of hCNs is described elsewhere (Bilican et al., 2014; James et al., 2014; Livesey et al., 2014).

2.2. Cooling Paradigm

Triplicate plates for each hCN batch were maintained in normal differentiation media. Hypothermia was induced at 5 wk when >90% of cultured cells are differentiated neurons and >95% of these fire action potentials (Bilican et al., 2014). Identical plates were separated and incubated at 28, 32 or 37°C to simulate 'moderate hypothermia', 'mild hypothermia' or 'normothermia' respectively (Rzechorzek et al., 2015). Hypothermic temperatures were selected to simulate suspended animation at the lower limit of cardiac stability and the minimum clinical target temperature for therapeutic hypothermia (Zell and Kurtz, 1985; Yenari and Han, 2012; Andrews et al., 2015). Thermic period was calibrated with a sentinel culture plate. Time zero was set when media in the sentinel plate reached the desired incubation temperature, measured by digital thermometer. Samples for early and late analysis of transcripts were captured for RNA extraction at 3 and 24 h respectively. At 24 h cells were fixed for immunocytochemistry and additional samples lifted for phospho-protein (see Supplemental Materials and Methods). For media additions during the hypothermic period, solutions were pre-warmed to the respective temperatures.

2.3. Electrophysiology

Whole-cell patch-clamp recordings were made from hCNs using an Axon Multiclamp 700B amplifier (Molecular Devices, Union City, CA). Patch electrodes (~4–7 MΩ) were filled with an internal recording solution comprising (in mM): K-gluconate 155, $MgCl_2$ 2, HEPES 10, Na-PiCreatine 10, Mg_2-ATP 2 and Na_3-guanosine triphosphate 0.3, pH 7.3 (300 mOsm). Coverslips containing hCNs were super-fused with an extracellular solution composed of (in mM) NaCl 152, KCl 2.8, HEPES 10, $CaCl_2$ 2, glucose 10, pH 7.3 (320–330 mOsm) using a gravity-feed system at room temperature (20–23 °C). The recording solution was supplemented with glycine (50 μM), picrotoxin (50 μM), strychnine (20 μM), and tetrodotoxin (300 nM). Recordings were made at a holding potential of −74 mV (including liquid junction potential correction). Series resistances (R_s) were generally less than 25 MΩ.

2.4. PP2A Enzyme Activity

PP2A activity was assayed using an Immunoprecipitation Phosphatase Assay Kit (Millipore) according to the manufacturer's instructions, with a few minor adaptations. Briefly, cell pellets from 5 wk old hCNs were thawed on ice, solubilised in cold phosphate extraction buffer (20 mM Imidazole-HCl (Santa Cruz), 2 mM EDTA, 2 mM EGTA, protease inhibitors and 100 μM PMSF) and sonicated for 10 s. After centrifugation (2000 ×*g* for 5 min at 4 °C), supernatants were collected and their protein concentration measured by BCA assay (Pierce). 100 μg of each lysate was incubated (constant rocking for 1 h at 4 °C) with an antibody specific to the active subunit of PP2A (Anti-PP2A, C subunit, clone 1D6) and Protein A agarose slurry in pNPP Ser/Thr Assay Buffer. Agarose beads were washed several times with TBS and Ser/Thr Assay Buffer before the addition of a Threonine Phosphopeptide (K-R-pT-I-R-R, final concentration 750 μM). Identical samples from each cortical batch were incubated for 10 min on a shaking incubator under one of 4 conditions (28, 32 or 37 °C or at 37 °C in the presence of 100 nM of fostriecin (CalBiochem)). After brief centrifugation, triplicate aliquots of each sample were transferred to a 96-well microtitre plate. Malachite Green Phosphate Detection Solution was added to each well and the plate incubated at room temperature for 15 min. Absorbance was measured on a spectrophotometer at 620 nm. Sample readings were compared to a 200–2000 pM Phosphate Standard Curve after subtraction of the blank (negative control) value. The specific PP2A activity (picomoles of phosphate released min^{-1} μg^{-1} protein) was calculated for each sample and its internal negative control (with fostriecin) so that this background 'activity' relating to residual phosphate levels could then be subtracted. Hypothermic sample values were then compared to their respective normothermic controls.

2.5. Statistical Analysis

Pairwise correlations were performed by two-tailed Pearson correlation. All remaining analyses were performed using linear mixed models in Stata SE (Version 9.2, Stata Corp, TX, USA) with random effects for intercept by batch, and where necessary, with random effects for coefficient by concentration or time (Aarts et al., 2014). *N* denotes the number of individual cell lines used and *n* describes the number of independently differentiated batches of hCNs. Unless otherwise stated, data are presented as standardized point estimates (SPE) + standardized estimated standard error (SESE) after normalizing to control values. Control values refer to aNPC, normothermia (37 °C) or untreated cells for differentiation, hypothermia, KCl/FPL stimulation and pharmacological studies respectively. In every case, asterisks denote significance of the test statistic as follows: $^{*}p < 0.05$, $^{**}p < 0.01$, $^{***}p < 0.001$, $^{****}p < 0.0005$.

3. Results

3.1. Tau Development in hCNs

Functional hCNs express an enriched cortical transcript profile (Espuny-Camacho et al., 2013; Bilican et al., 2014; Livesey et al., 2014), display axonal-dendritic polarization and exhibit ultrastructural synaptic morphology (see Fig. S1). However tau modulation – a key feature of neuronal development – has not previously been explored in this system. In the adult human brain, six major tau isoforms arise from alternative splicing of the gene *MAPT* (Goedert et al., 1989a). These isoforms differ by their number of repeated microtubule binding domains; three repeat (3R) tau predominates during early development, whilst approximately equal levels of 3R and 4R tau exist in the mature brain (Goedert et al., 1989b; Goedert and Jakes, 1990). To determine whether hCN differentiation reflects normal developmental changes in tau, we examined neurons at serial time points from 1 to 7 wk after plating. Early tau development was recapitulated at transcript level with significant increases in total, 3R and 4R tau expression during differentiation of independent hES and iPS-derived hCNs (Fig. 1A). A shift in 3R:4R ratio between wk 4 and 7 partially mimicked the transition from human foetal to adult brain (Fig. 1B). Tau protein was not detected in neural precursors (Fig. 1C). Dephosphorylation of soluble cell lysates prior to SDS-PAGE produced a clear shift in electrophoretic mobility and resolved the tau signal at wk 4 and 6 into a single band, corresponding to foetal isoform 3R0N (Goedert et al., 1989b) (Fig. 1C). Immunocytochemistry confirmed a prominent 3R tau expression and an increase in the proportion of hCNs expressing tau during differentiation (Fig. 1D–E). Further, it showed a cell soma-restricted expression of protein detected with a 4R human tau-specific antibody by wk 4 (Fig. 1D), which extended further into neuronal processes by wk 7 (Fig. 1F).

Alongside splicing regulation, tau becomes progressively dephosphorylated during development, increasing its affinity for microtubules (Gong et al., 2000). This is attributed to increased expression of PP2A — the principal tau phosphatase in the human brain (Yu et al., 2009). Foetal brain tau is thus more highly phosphorylated than adult brain tau, but both become dephosphorylated in post-mortem samples due to residual PP2A activity (Brion et al., 1993; Matsuo et al., 1994) (Fig. 2A–B). Reflecting their early developmental state, tau phosphorylation (and electrophoretic mobility) in hCNs under basal conditions was similar to that observed in primary cultures derived from human foetal cortical samples (Fig. 2B). Tau phosphorylation at several epitopes decreased between wk 4 and 6 of differentiation (Fig. 2C–D), coinciding with an increase in PP2A mRNA expression (Fig. 2E). Importantly, tau was absent in negative control samples (primary human and hiPS-derived astroglia) but was identified in oligodendroglia (Lopresti et al., 1995) within primary mixed glial cultures derived from human foetal ventral telencephalon (Fig. 2F–G). In summary, tau modifications with respect to both 3R:4R ratio and phosphorylation during differentiation of hCNs recapitulate features of early in vivo human cortical tau development. In this regard, hCN cultures offer a suitable platform for exploring human tau physiology under hypothermic conditions.

3.2. Cooling Reverts Tau to an Earlier Developmental State

Brain tau protein in rodent models becomes increasingly and reversibly phosphorylated with decreasing temperature, consistent with recapitulation of a "foetal-like" state (Mawal-Dewan et al., 1994; Stieler et al., 2011). To determine whether hypothermia modifies tau dynamics in functional human neurons we evaluated tau isoform transcripts in wk 5 hCNs following hypothermic incubation for 24 h. An increase in 3R:4R tau ratio was observed with cooling, most notably at 32 °C (32 °C, $P < 0.0005$ and 28 °C, $P = 0.012$, Fig. 3A–D). This shift reflected a significant increase in 3R tau transcript at both hypothermic temperatures ($P < 0.01$) and a reduction in 4R tau transcript at 32 °C ($P = 0.009$, Fig. 3A–D). Total tau transcript expression and transcript N-terminal length remained stable across temperatures (Figs. 3B and S2). Western blot analysis confirmed an increase in 3R tau protein expression at 28 °C ($P = 0.011$), alongside a decrease in electrophoretic mobility, but no detectable change in tau solubility (Figs. 3E and S2). Quantitative immunolabelling revealed a 35% reduction in 4R tau-positive cells at 32 °C (Fig. 3F–G, $P = 0.017$). These results are consistent with cooling-induced reversal of tau isoform and post-translational state, without the oligomerization typically assigned to 'pathological tau' (Spillantini and Goedert, 2013).

We further characterized post-translational effects of cooling by immunocytochemistry and quantitative Western analysis of tau phosphorylation at the AT8 epitope (pSer202/pThr205). AT8 is heavily phosphorylated in the foetal and diseased adult human brain, as well as hypothermic rodent models (Planel et al., 2007). At 24 h we noted a temperature-dependent increase in AT8 expression with cooling according to Western analysis (normalized to total tau expression; 32 °C $P = 0.004$, 28 °C $P < 0.0005$) and cell counts (32 °C $P = 0.008$, 28 °C $P < 0.001$) (Fig. 4A–C). A similar increase in phosphorylation (normalized to total tau expression) was seen at other phospho-tau epitopes associated with pathological tau (PHF-1 $P < 0.05$, AT180 $P < 0.01$, AT270 $P < 0.0005$, Fig. 4D) including AT100 (see Fig. S3). In hypothermic rodents, a disproportionate inhibition of tau phosphatase activity (relative to tau kinase activity) is thought to underlie a hypothermic increase in tau phosphorylation (Planel et al., 2004). In hCNs, no difference was seen in PP2A-Bγ transcript (not shown) or in protein levels of the active subunit of PP2A (PP2A-C) with temperature shift (Fig. 4E). To evaluate phosphatase activity, we immunoprecipitated PP2A-C from wk 5 cultures and measured the ability of this isolate to release phosphate from a threonine phosphopeptide (K-R-pT-I-R-R) at the 3 temperatures of interest over a 10 min period. As an additional negative control, a sample of isolated PP2A-C from each hCN batch was simultaneously incubated at 37 °C in the presence of fostriecin (a selective inhibitor of PP2A (Walsh et al., 1997)) — the resultant background phosphate level was subtracted from the test lysates. Both mild and moderate hypothermia produced a >60 % reduction in PP2A-C activity (32 °C $P = 0.041$, 28 °C $P = 0.034$, Fig. 4F). Together these findings reveal that hypothermia induces reversal of key tau ontogenic features and impairs tau phosphatase activity in human cortical neurons in vitro.

3.3. Hypothermia Reduces Oxidative and Excitotoxic Injury in hCNs

Identical hCN batches were cultured at three different temperatures (28 °C, 32 °C and normothermia (37 °C)) to demonstrate the neuroprotective effect of hypothermia against oxidative stress. Temperature shift alone did not affect hCN viability or culture purity (Fig. S4). To avoid a confounding cellular stress by re-warming, we pre-cooled hCNs for 24 h then maintained them at their respective temperatures throughout exposure to stressors in minimal medium (MiM) (Lleonart, 2010; Chip et al., 2011). The combined cooling and stress paradigm is summarized in Fig. 5A. 24 h treatment with H_2O_2 produced concentration-dependent injury according to multiplexed injury analysis (Rzechorzek et al., 2015) and cell death counts (Fig. 5B–E). Hypothermia was neuroprotective; injury in response to 100 μM H_2O_2 treatment was reduced by 36% at 32 °C (19.9% versus 31.3% at 37 °C, $P = 0.046$) and 78% at 28 °C (6.9% versus 31.3%, $P < 0.0005$) (Fig. 5B). Cell death counts reflected the injury data (reduction at 32 °C, 14.6%, $P = 0.013$, and at 28 °C, 29.2%, $P < 0.0005$, Fig. 5C).

To determine whether cooling protected hCNs against another common neuronal stressor, we examined the effect of hypothermia on glutamate-mediated excitotoxicity (Gupta et al., 2013). Neurons cultured in MiM were vulnerable to concentration-dependent glutamate toxicity (Fig. 6A). Cooling was again protective; cell injury following exposure to 30 μM glutamate was reduced by 25% at 32 °C and 56% at 28 °C (51.4% and 29.9% injury respectively versus 68.6% injury at 37 °C, $P < 0.0005$ for both comparisons). To verify the physiological relevance of this excitotoxic response, we established that it was abolished at each

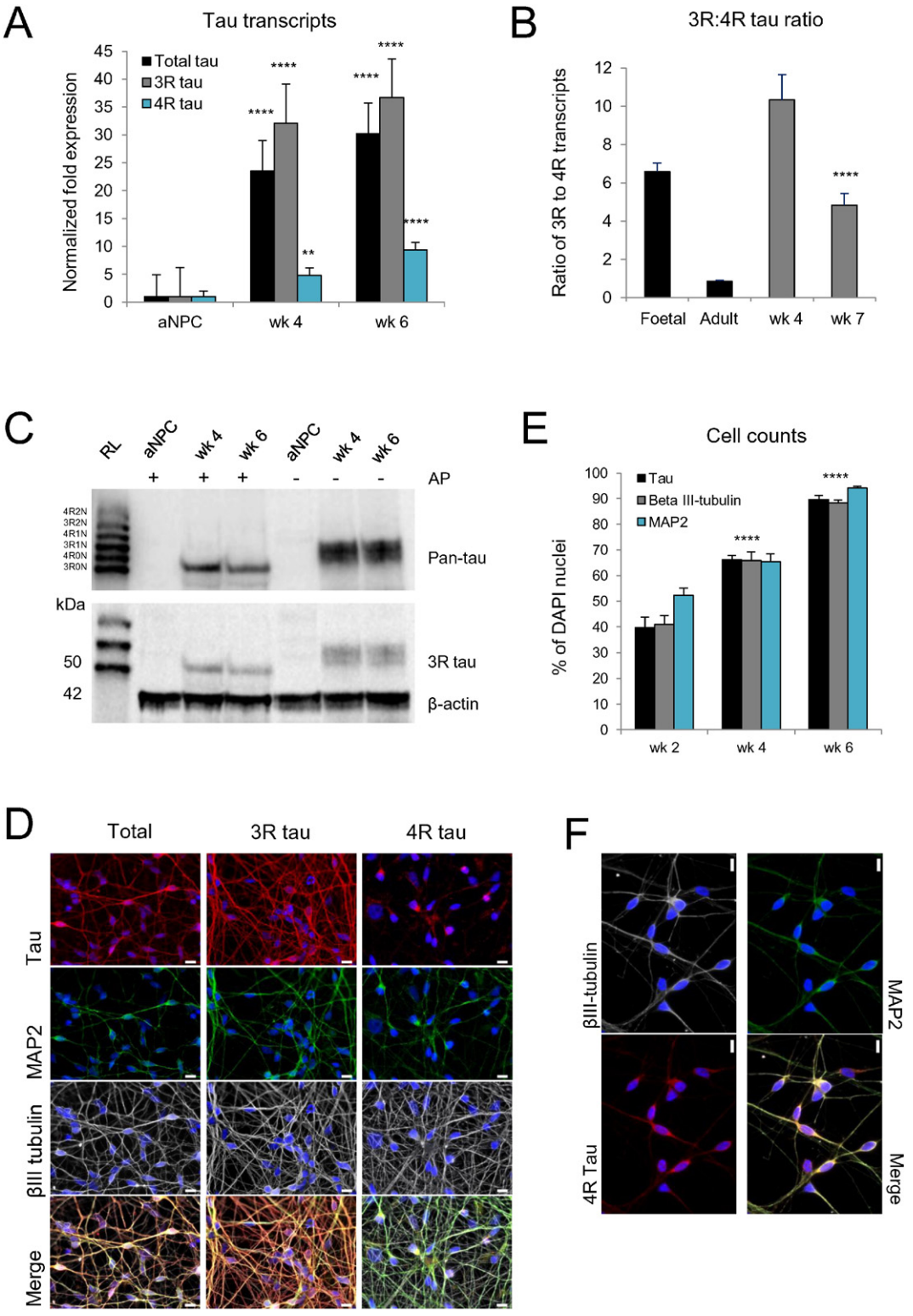

Fig. 1. Differentiating hCNs recapitulate early human tau development. (A) q-RT-PCR analysis of total, 3R and 4R tau transcripts from aNPC stage to wk 6 ($N = 2$; $n = 5$; HES1 $n = 4$, IPS1 $n = 1$; 4R tau at 4 wk $P = 0.005$, other increases $P < 0.0005$). (B) Shift in tau isoform ratio between wk 4 and 7 ($N = 1$; HES1 $n = 5$; $P < 0.0005$), partially mimics transition from human foetal to adult brain (triplicate cDNA synthesised from commercially pooled RNA). Transcript data normalized to geometric mean of 3 differentiation-stable reference targets then presented as SPE + SESE relative to aNPC expression (for hCNs) or mean of triplicates + SEM (for pooled human brain). (C) Western blot of soluble tau during hCN differentiation, run by 10% SDS-PAGE with (+) or without (−) prior dephosphorylation with alkaline phosphatase (AP). Blot probed with pan-tau antibody (upper image) recognising all tau isoforms irrespective of phosphorylation status. Positive control includes recombinant human tau protein ladder (RT) containing 6 human brain tau isoforms. Membrane re-probed with 3R tau-specific antibody RD3 (lower image). β-actin = loading control. (D) Fluorescent micrographs of hCNs (IPS1) at wk 4, co-stained for DAPI, neuronal markers (microtubule-associated protein 2 (MAP2) and βIII-tubulin) and tau (pan-tau, 3R- or 4R-specific). Somatic-axonal distribution of 3R and total tau reflects developing polarity, scale bar = 10 μm. (E) Quantification of hCN protein expression by immunolabelling, asterisks denote significant changes relative to wk 2 post-plating ($N = 3$; $n \geq 4$; HES1 $n \geq 2$, IPS1 $n \geq 1$, IPS2 $n \geq 1$, $P < 0.0005$). Cell counts presented as mean + SEM. (F) Fluorescent micrographs of hCNs 53 d post-plating showing more extensive 4R tau staining (scale bar = 10 μm). See also Fig. S1.

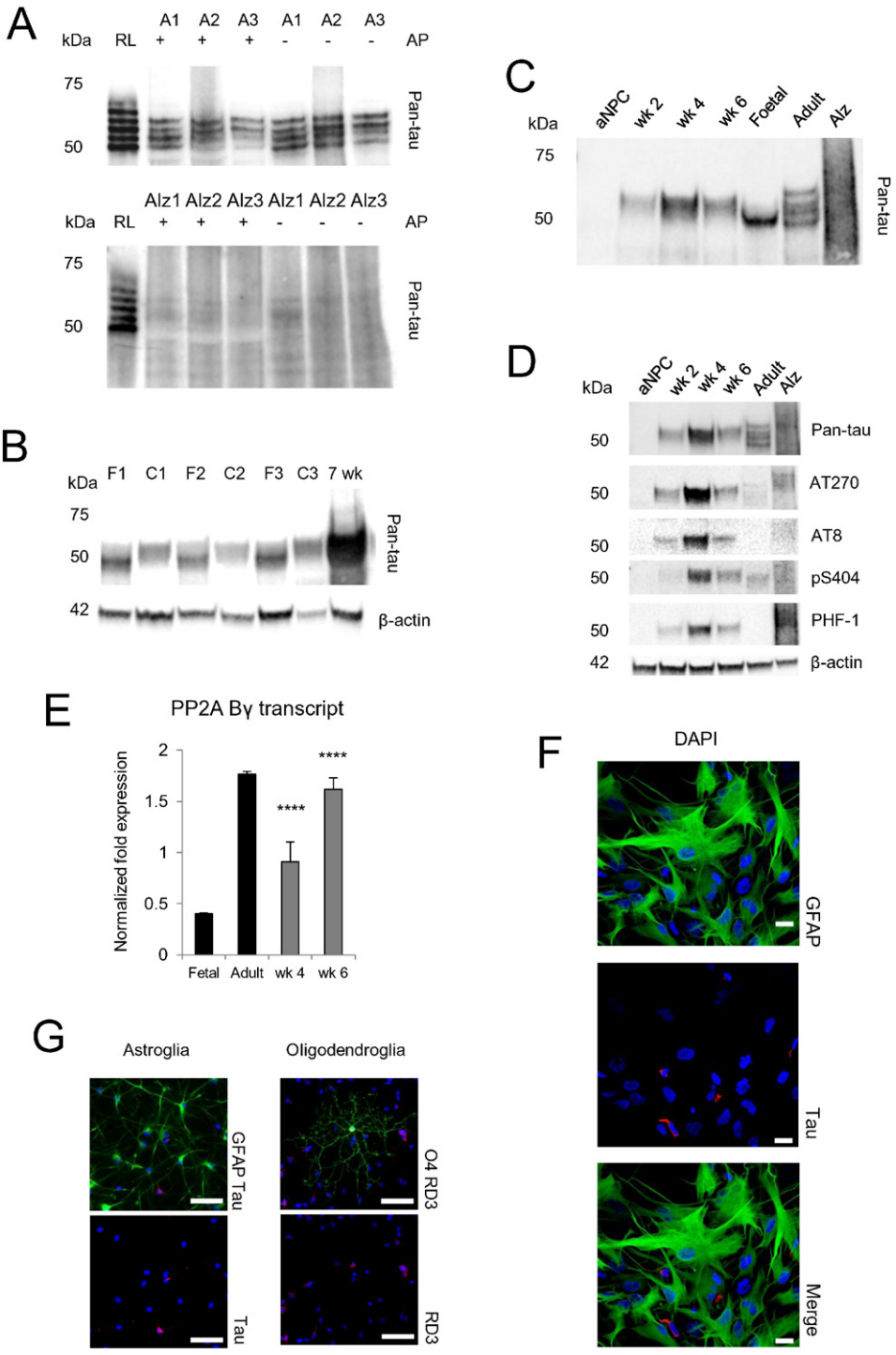

Fig. 2. Phospho-tau expression in differentiating hCNs. (A) Soluble tau expression in human post-mortem cortical tissue samples. Upper blot: 3 independent adult control samples (A1, A2, A3 ages 17, 44 and 75 yr. respectively) — note multiple tau isoforms and lack of tau mobility shift after AP treatment demonstrating low phosphorylation status after post-mortem interval (PMI) (Matsuo et al., 1994). RL = recombinant human tau ladder. Lower blot: 3 independent Alzheimer disease samples (Alz1, Alz2, Alz3 ages 60, 61 and 81 yr. and Braak stages 6, 5 and 6 respectively), note tau 'smears' indicating oligomerization with reduced solubility compared to control samples. Poor electrophoretic mobility indicates hyperphosphorylated and multimeric state that cannot be altered by AP treatment and is relatively unaffected by PMI. (B) Comparison of soluble tau expression in mature hCNs and human foetal cortex. 3 independent foetal cortical samples (F1, F2, F3 at 14, 15 and 16 wk gestation respectively) and primary cultures derived from these samples (C1, C2, C3 respectively) (see Supplemental Materials and Methods). 7 wk = hCNs at 7 wk post-plating. Note mobility shift between tissue and culture samples, indicating that PMI allows continued dephosphorylation of tissue samples prior to processing. Note that 7 wk hCN tau aligns with primary culture tau. Blot probed with pan-tau antibody that recognises both phosphorylated and dephosphorylated tau. (C) Soluble phospho-tau expression during hCN differentiation. Blot shows total tau in aNPCs and hCNs at various points during differentiation (2, 4 and 6 wk post-plating) as compared to foetal cortical sample at 19 wk gestation, adult control cortex, and Alzheimer disease (Alz) cortex. Note expression in 4 wk hCNs is greater than at 6 wk and in foetal and adult samples but is similar to Alz. Foetal sample sits at lower molecular weight than hCN samples even without AP treatment, indicating lower phosphorylation status due to PMI. (D) Western blots probed with antibodies specific for tau phospho-epitopes. Note decrease in signal at each epitope between wk 4 and 6 of hCN differentiation, weak signal in normal adult human cortex (age 17 yr) and prominent signal in Alz-affected cortex (age 60 yr., Braak stage 6). Note AT8 and AT270 signals are less than PHF-1 in the diseased sample, reflecting order in which any remaining soluble tau becomes dephosphorylated during PMI (Matsuo et al., 1994), despite low PP2A expression (see Fig. 4E). (E) PP2A Bγ transcript changes in hCNs ($N = 2$; $n = 5$; HES1 $n = 4$, IPS1 $n = 1$, $P < 0.005$) echo human brain development. (F) Confocal image of hPS-derived astrocytes, negative for tau (scale bar = 10 μm). (G) Fluorescent micrographs of astrocytes (left) and oligodendroglia (right) in mixed primary cultures derived from 19 wk post-mortem foetal ventral telencephalon. Note somatic 3R tau (RD3) expression in O4-positive oligodendroglia but absence of tau in GFAP-positive astroglia, scale bar = 50 μm.

temperature through antagonism of N-methyl-D-aspartate receptors (NMDARs), principally composed of GluN1/GluN2B subunits (Fig. 6A–B). With absolute cell death counts protection was evident at 32 °C (20.5% versus 30.1% death at 37 °C, $P = 0.001$), but not at 28 °C (28.8% death, $P = 0.654$) (Fig. 6C–D). Taken together, these results confirm that mild-to-moderate hypothermia protects human cortical neurons from both oxidative and glutamate-mediated injury in vitro.

3.4. PP2A Inhibition Increases Tau Phosphorylation and Reduces Oxidative Injury in Normothermic hCNs

Tau hyperphosphorylation may offer short-term protection by promoting apoptotic escape (Liu et al., 2012). Since hypothermia robustly increased tau phosphorylation in hCNs, we postulated that this might contribute to its neuroprotective effect. First we determined whether

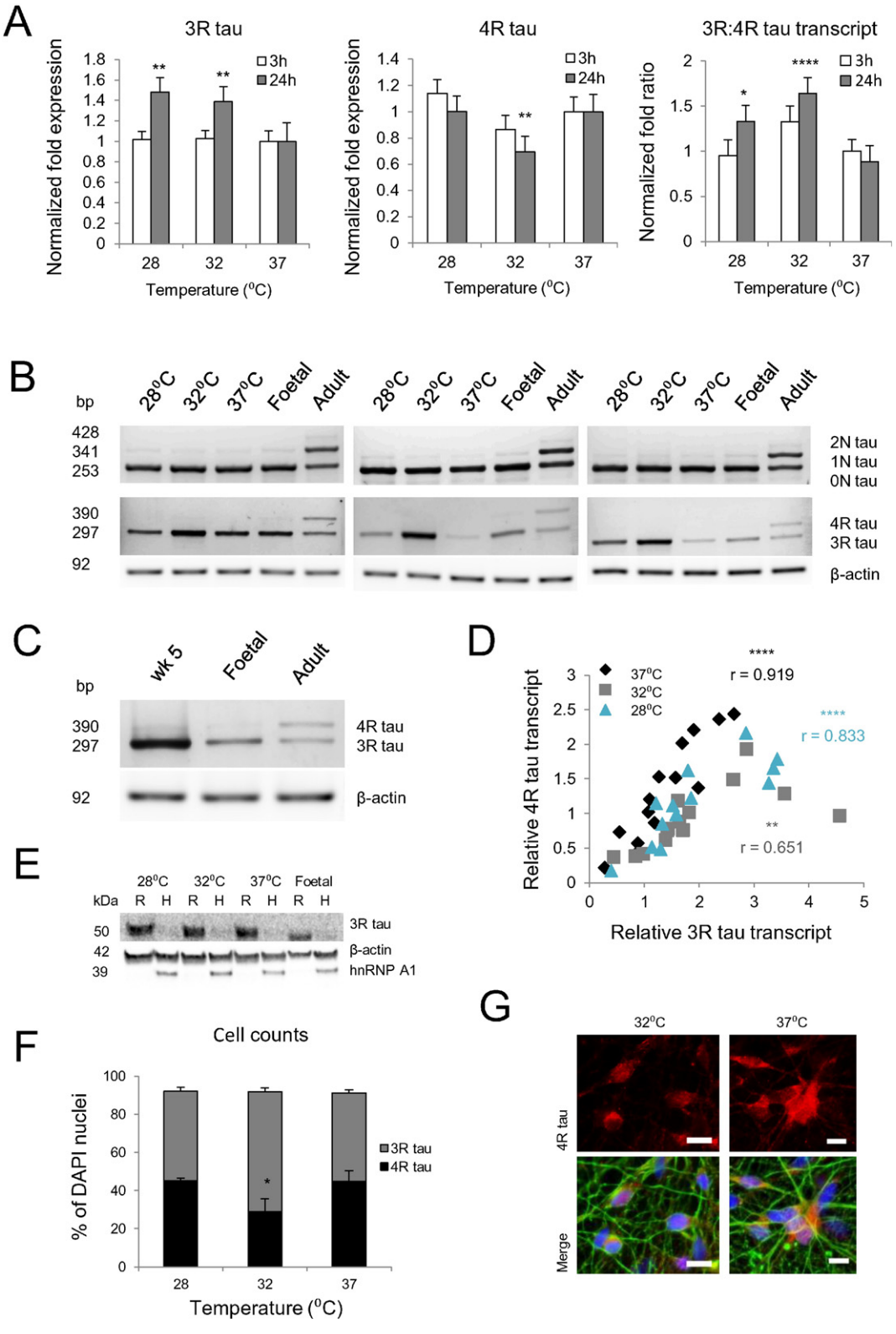

neuroprotection could be achieved by inhibiting PP2A. Fostriecin was applied to normothermic hCNs for 24 h, after which cells were immunostained, harvested for protein extraction or subjected to oxidative stress. Fostriecin treatment produced a visible increase in axonal AT8 immunoreactivity, a concentration-dependent increase in phospho-tau signal on Western blot and a reduction in hCN injury in response to H_2O_2 ($P = 0.008$, Fig. 7A–C). Culture at 28 °C predictably reduced oxidative stress-mediated injury across all H_2O_2 doses ($P < 0.0005$), however the addition of fostriecin conferred no further benefit ($P = 0.907$, Fig. 7C). Conversely, treatment with the kinase inhibitor TCS 2002 (highly selective for the major tau kinase GSK3β (Saitoh et al., 2009)) produced a concentration-dependent decrease in phospho-tau signal as well as a prominent shift in electrophoretic mobility on Western blot (Fig. 7B). Addition of TCS 2002 increased hCN injury in response to H_2O_2 under both normothermic and hypothermic conditions ($P = 0.002$ and $P = 0.001$ respectively, Fig. 7D). TCS 2002 abrogated the protective effect of moderate hypothermia at 50 μM H_2O_2; there was no significant difference between injury in untreated normothermic cultures and hypothermic cultures treated with TCS 2002 ($P = 0.348$). Importantly, expression of the activated form of GSK3β was unaffected by cooling, confirming the availability of this enzyme for TCS 2002 inhibition at 28 °C (Fig. 7E). Finally, immunolabelling of hCNs for activated caspase-3 and AT8 showed that these markers were mutually exclusive, suggesting that phospho-tau positive neurons were resistant to apoptosis (Li et al., 2007) (Fig. 7F). In summary, these findings are consistent with a rapid, cooling-induced hyperphosphorylation of tau, coupled with a potent defence of human cortical neurons against acute oxidative injury. Our results further indicate that this protective effect is saturated at 28 °C.

4. Discussion

This study establishes an in vitro model of hypothermic tau modulation in human cortical neurons. hCNs respond robustly to cooling, with changes in tau at transcript, protein and post-translational levels, consistent with reversal of ontogenic transitions in tau status observed during differentiation. Hypothermia also prevents hCN injury in response to exogenous stressors, operating in a temperature- and stress-specific manner. Finally we show that hypothermic neuroprotection is impaired at 28 °C and mimicked at 37 °C using compounds that reciprocally modify tau phosphorylation. Our results provide further evidence that phospho-tau may participate in a neuroprotective response, and that our translatable cooling paradigm offers a simple tool with which to test this hypothesis in future studies.

Temporal analysis of hCN differentiation captured fundamental aspects of early human cortical tau development, including a shift in tau isoform ratio and a parallel decrease in tau phosphorylation. Even at later time points, hCN tau was more phosphorylated than that extracted from human adult and foetal cortical tissue (Fig. 2C–D). Comparison of phosphorylation status in post-mortem samples and hCNs is confounded by PMI, during which residual PP2A activity can take effect (Matsuo et al., 1994). In support of this, tau phosphorylation was reduced in foetal human post-mortem cortices relative to primary cultures derived from these samples (Fig. 2B). Despite a considerable PMI, tau extracted from adult human pathological samples remained hyperphosphorylated (Fig. 2A and C–D), likely due to reduced PP2A expression (Fig. 3E) or shielding of phospho-epitopes within multimeric insoluble tau species (Fig. 2A). An unresolved challenge is to derive a protocol that efficiently and reproducibly generates wild-type human neurons with a mature tau profile. As found in other human in vitro systems (Sposito et al., 2015), our hCNs are limited with respect to biochemical analysis of tau isoforms, complicated by sparse availability of 4R tau-specific antibodies. One possible explanation for the discrepancy between our immunocytochemical and biochemical readouts for 4R tau protein in hCNs is that this target resided in a relatively insoluble fraction, ineffectively extracted prior to SDS-PAGE. Despite these caveats, the data above shows that hCNs can be used to study aspects of developing tau physiology in a clinically-relevant context. Indeed, an immature profile may be desirable for modelling therapeutic hypothermia — an intervention most widely used to treat hypoxic ischaemic neonatal encephalopathy (Yenari and Han, 2012; Jacobs et al., 2013). Hypothermia reversed the principal features of tau development observed during hCN differentiation, pushing tau towards an earlier ontogenic state. Tau thus became hyperphosphorylated with a significant reduction in PP2A activity at low temperatures. This hypothermic modulation of PP2A appears to outweigh any hypothermic inactivation of tau kinases (Fig. 7E) as described in other systems (Planel et al., 2004; Bretteville et al., 2012). Accordingly, we found that TCS 2002 (but not fostriecin) impacted upon hCN injury at 28 °C, suggesting a residual GSK3β (but not PP2A) activity at this temperature. In addition, we noted a hypothermic shift in tau isoform ratio with a decrease in 4R tau expression at 32 °C. Further work is needed to identify the mechanism(s) responsible for tau splicing shift in response to cold-stress, and whether this requires associated changes in the expression or distribution of tau splicing regulators.

In agreement with others, we found that short periods of hypothermia have negligible effect on basal viability, but reduce cell injury in the face of oxidative stress (Antonic et al., 2014; Rzechorzek et al., 2015). Our multiplexed injury analysis (Rzechorzek et al., 2015) also addresses previous limitations including the impact of cell number variability across treatment conditions (Antonic et al., 2014). Hypothermic protection of hCNs from glutamate-mediated cell death was temperature-specific (Fig. 6C), whereas that from glutamate-induced cellular injury was temperature-dependent (Fig. 6A). Resolving cytotoxicity and viability data (Fig. S5) shows that, despite a temperature-dependent decrease in lactate dehydrogenase (LDH) release, ATP production was similar at both hypothermic temperatures. Cell death counts were however lowest at 32 °C. One interpretation is that moderate hypothermia affected lipid bilayer structure (Lleonart, 2010) thus preventing LDH release. However, viability may have also been underestimated if hypothermia affected enzymatic production of ATP. Another confounding factor might be residual precursor proliferation at higher temperatures compared to cell cycle arrest at 28 °C (Lleonart, 2010). Our cell

Fig. 3. Hypothermia reverses tau isoform shift in hCNs. (A) q-RT-PCR analysis of transcripts in wk 5 hCNs ($N = 3$; $n = 14$; HES1 $n = 7$, HES2 $n = 4$, IPS1 $n = 3$) after 24 h temperature shift showing significant increase in 3R tau at both hypothermic temperatures (left). Note also a late decrease in 4R tau expression at 32 °C (middle). At 24 h this produces a shift in tau isoform ratio (right). Transcript data normalized to geometric mean of 2 temperature-stable reference targets then to normothermic control at each time point. Note that 3R/4R transcript ratio is displayed as fold change relative to normothermic control ratio at 3 h. (B) Qualitative RT-PCR products generated with tau exon spanning primers (see Supplemental Materials and Methods) from 3 independent batches of hCNs (left to right; HES1 $n = 2$; HES2 $n = 1$) after 24 h culture at 3 different temperatures, as compared to human foetal and adult brain. Upper panel shows products obtained with primers that span tau exons 1 to 5, thus amplifying transcripts of variable N-terminal length. Note predominant expression of 0 N transcripts in both hCNs and foetal brain with low expression of 1 N isoforms, and approximately equal expression of 0 N and 1 N transcripts in adult brain with low expression of 2 N species. No obvious effects of temperature shift on N-terminal length are noted. Lower panel shows products obtained with primers that span tau exons 9–11, thus amplifying transcripts with or without tau exon 10 (4R or 3R tau respectively). Note roughly equal expression of 3R and 4R tau in human adult brain and predominance of 3R tau species in both hCNs and human foetal brain. There is a clear increase in 3R transcript expression at 32 °C, consistent with q-RT-PCR results. This increase saturates the signal, making it difficult to visualise the low expression of 4R tau in hCNs at any temperature. 4R tau expression is however notable in (C) where similar products from normothermic wk 5 hCNs (HES1) were analysed without temperature-shifted cells. Note that the ratio of 3R to 4R expression in these hCNs approximates to 8:1, consistent with that predicted from q-RT-PCR results in Fig. 1B. β-actin serves as a housekeeping target in both (B) and (C). (D) Two-tailed Pearson correlation illustrates dissociation of relationship between 3R and 4R tau transcripts at 32 °C (28 °C $P < 0.0005$, 32 °C $P = 0.012$, 37 °C $P < 0.0005$). (E) Representative blot depicts upward mobility shift of 3R tau in hypothermic cultures. 3R tau solubility was unaffected (3R tau found in RIPA-soluble fraction (R) but absent from high detergent fraction (H); β-actin and heterogeneous nuclear ribonucleoprotein (hnRNP) A1 serve as cytosolic and nuclear loading controls respectively. (F) Cell counts show reduction in 4R tau expression at 32 °C ($N = 2$; $n = 4$; HES1 $n = 3$, IPS1 $n = 1$), depicted in fluorescent micrographs in (G), merged images show co-staining for DAPI and βIII-tubulin, scale bar = 10 μm. See also Fig. S2.

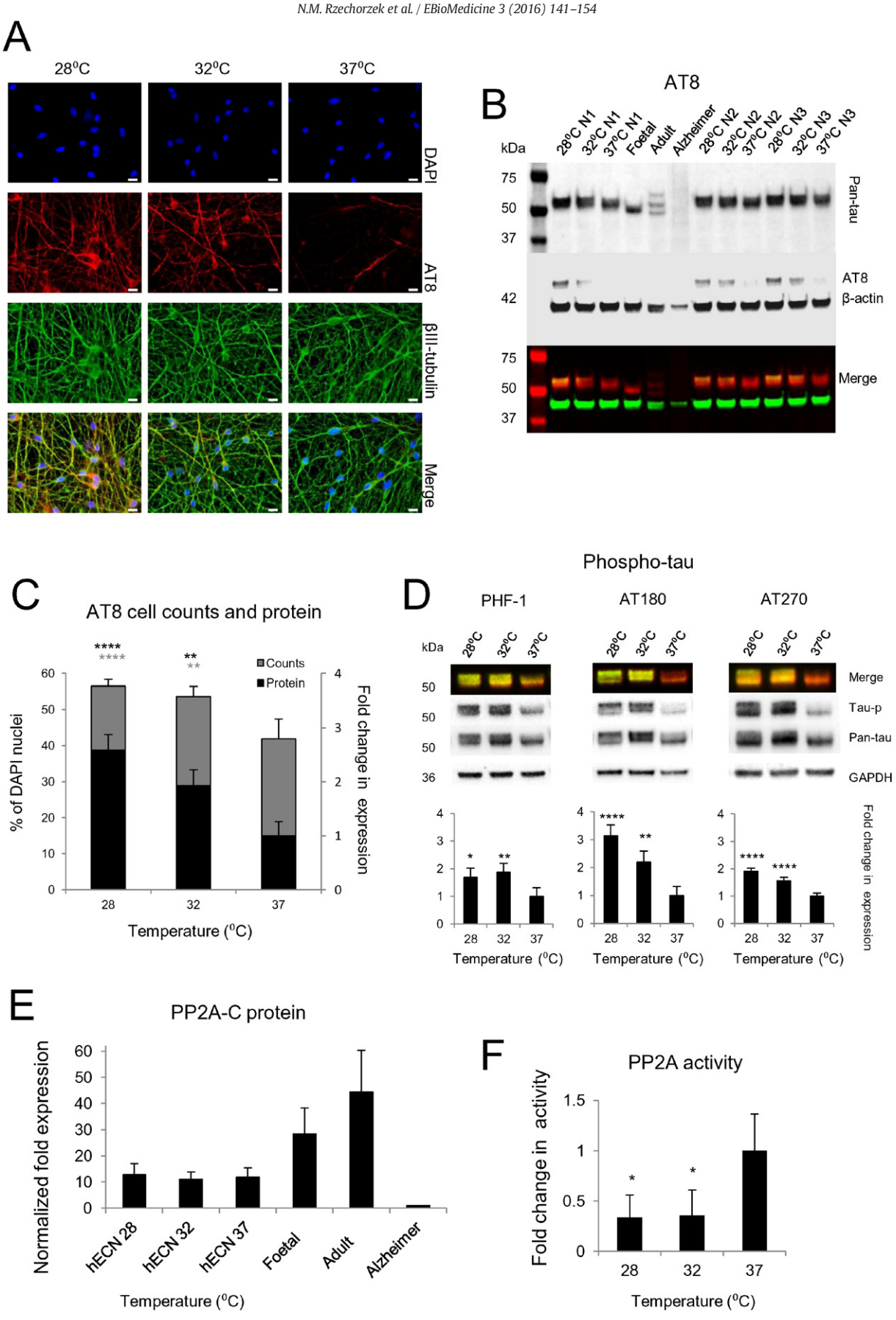
A
28°C
32°C
37°C
DAPI
AT8
βIII-tubulin
Merge
B
AT8
kDa
28°C N1
32°C N1
37°C N1
Foetal
Adult
Alzheimer
28°C N2
32°C N2
37°C N2
28°C N3
32°C N3
37°C N3
75
50
37
Pan-tau
42
AT8
β-actin
Merge
C
AT8 cell counts and protein
Counts
Protein
% of DAPI nuclei
Fold change in expression
Temperature (°C)
D
Phospho-tau
PHF-1
AT180
AT270
Merge
Tau-p
Pan-tau
GAPDH
Fold change in expression
Temperature (°C)
E
PP2A-C protein
Normalized fold expression
hECN 28
hECN 32
hECN 37
Foetal
Adult
Alzheimer
Temperature (°C)
F
PP2A activity
Fold change in activity
Temperature (°C)

count data is thus complementary to, but distinct from our multiplexed injury analysis, which offers an additional, objective assessment of culture health (Rzechorzek et al., 2015). Overall we have demonstrated that hypothermia protects human cortical neurons in vitro from glutamate-mediated excitotoxicity, in addition to oxidative stress (Rzechorzek et al., 2015) – key components of both acute and chronic neuronal injury.

The molecular mechanisms underlying hypothermic neuroprotection are ill-defined, although several pathways are implicated in other model systems and within the cyclical adaptation of hibernating brains (Arendt et al., 2003; Stieler et al., 2011; Yenari and Han, 2012; Peretti et al., 2015; Zhu et al., 2015). Direct effects such as a reduced rate of generation of oxidative species and changes in glutamate receptor function may be involved in hypothermic neuroprotection against oxidative and excitotoxic stress respectively (Dietrich et al., 2009). In addition, tempering either one of these stressors directly may have indirect benefits with respect to the other. For example, modulation of synaptic activity can increase antioxidant capacity (Papadia et al., 2008) and hypothermia can reduce ischaemia-induced glutamate release (Busto et al., 1989). Cold-shock proteins are also emerging as critical regulators of hypothermic neuroprotection (Peretti et al., 2015; Zhu et al., 2015) and these factors may feature significantly in the hypothermic preconditioning of hCNs (Rzechorzek et al., 2015). Of particular relevance to our current work is that the synaptic plasticity of hibernation has been linked to modification of tau, in a manner that closely resembles hypothermic transitions in hCNs (Arendt et al., 2003). The re-acquisition of a primitive tau status could offer multiple benefits such as potentiation of hCN tolerance to glutamate. Interestingly, a negative feedback loop has been described in which tau phosphorylation responds to NMDAR activity and subsequently prevents 'overexcitation' (Mondragon-Rodriguez et al., 2012). Our results suggest that tau isoform balance in particular may influence the ability of hCNs to withstand excitotoxic insults. This would argue for isoform-specific roles of tau in synaptic homeostasis and would further advocate human modelling of neuronal injury. 4R tau reduction might also be essential when phosphorylation state is high, minimising available sites for excessive phosphorylation and subsequent aggregation. Ultimately, reduced 4R tau alongside increased tau phosphorylation might confer a more plastic cytoarchitecture — a prerequisite for repair or reorganisation.

Injury was unchanged in the presence of fostriecin under hypothermic conditions. This highlights the potency of cooling-induced PP2A suppression and suggests that tau phosphorylation was saturated at this temperature. Concurrently, inhibiting tau phosphorylation had the opposite effect to fostriecin, preventing the protection that would have otherwise been achieved at 28 °C. It must be noted that both PP2A and GSK3β have multiple protein targets other than tau that may have contributed to (or indeed driven) the protective effects noted in this study. However, emerging evidence suggests that tau hyperphosphorylation might promote apoptotic escape (Liu et al., 2012; see also Fig. 7F), pointing to a specific enrolment of phospho-tau in hypothermic neuroprotection. We recently reported that hypothermia primes proteostatic pathways in hCNs, thus providing 'cross-tolerance' to multiple stressors (Rzechorzek et al., 2015). The trigger for this preconditioning response remains to be identified, but given its rapid emergence in response to cooling, its association with endoplasmic reticulum stress (Iqbal et al., 2009) and its capacity to elicit an unfolded protein response (Liu et al., 2012), hyperphosphorylated tau represents an attractive candidate. Extending our knowledge of the preconditioning phase is a potentially fruitful avenue for targeting the earliest stages of neurodegenerative disease, in which the role of tau remains poorly understood. Based on the data provided above, we conclude that over a 48 h period of cooling, hyperphosphorylation of tau was correlated with neuronal protection rather than neuronal injury.

Historically, increased tau phosphorylation has been associated with neural demise. Consequently, rodent studies exploring increased neurofibrillary pathology after exposure to cooling-re-warming paradigms have linked this pathological risk with hypothermic hyperphosphorylation of tau (Planel et al., 2009). On the contrary, by excluding a re-warming phase (and the rebound cellular stress that might ensue (Lleonart, 2010; Rzechorzek et al., 2015)), our work indicates that real-time tau transitions under hypothermia do not negate its protective effect and may promote neuronal survival. In hCNs, tau responses to cooling extended to alternative splicing of *MAPT*, in a manner that complements the developmental reversal of tau phosphorylation state. This may be an essential feature of hypothermic tau in human neurons that simultaneously permits cytoskeletal plasticity whilst retaining tau solubility. Whilst it is tempting to speculate that cooling could impart a therapeutically-tractable, 'neonatal' plasticity to the adult brain, the effect of hypothermia on mature human tau isoforms is currently unknown. It must also be considered that increased plasticity within established networks may be undesirable in terms of cognitive outcome, even if it provides a neuroprotective benefit overall. Notwithstanding these caveats, our work fundamentally explores the molecular basis of hypothermic neuroprotection under 'ideal' circumstances — i.e. those in which neuronal temperature can be directly measured and controlled prior to and during the injury phase without the confounding effects of rewarming and other practical drawbacks (and risks) of clinical cooling. This approach not only lends itself to drug discovery (circumventing the need to cool patients), it raises the prospect of pharmacologically retaining protective factors that might otherwise be reversed upon rewarming. Manipulation of tau phosphorylation in the context of both cooling and injury has yielded the clearest evidence to date that protection of human neurons against oxidative stress is not impeded by tau hyperphosphorylation in the acute phase. Whether this would hold in the long term, or indeed whether tau is specifically contributing to hypothermic neuroprotection is yet to be determined in our system. Overall, these findings argue for further study of hypothermic preconditioning and context-dependent tau modulation to exploit their neuroprotective potential.

Author Contributions

Conceptualization, N.M.R.; Methodology, N.M.R, P.C. and M.R.L.; Investigation, N.M.R. and M.R.L.; Formal Analysis, P.C.; Writing – Original Draft, N.M.R.; Writing – Review & Editing, N.M.R., P.C., M.R.L., R.P., S.B., K.B., D.S., D.J.A.W., G.E.H. and S.C.; Funding Acquisition, N.M.R., P.C. and S.C.; Resources, P.C., S.B., K.B., D.S., D.J.A.W. and S.C.; Supervision, G.E.H. and S.C.

Fig. 4. Hypothermia inhibits PP2A and increases tau phosphorylation in hCNs.(A) Representative images of AT8 expression at 3 temperatures, scale bar = 10 μm. (B) Western blot showing increased phospho-tau (AT8) with hypothermia. β-actin = loading control, for multiplexed image AT8 and β-actin were imaged in 800 nm channel (green) and total tau in 700 nm channel (red). Note apparent lower phosphorylation state of post-mortem samples (foetal, adult, Alzheimer) due to PMI and because only soluble protein was loaded (most AT8 signal would be contained within the insoluble fraction which was not assessed). Note also that Alzheimer sample has been loaded at a lower total protein concentration to avoid oversaturation of signal for quantification of other lanes. (C) Western blot quantification of AT8 expression, normalized to total tau ($N = 3$; $n = 6$; HES1 $n = 4$, HES2 $n = 1$, IPS1 $n = 1$) and quantification by cell count ($N = 3$; $n = 6$; HES1 $n = 3$, HES2 $n = 2$, IPS1 $n = 1$). Cell count data are presented as mean + SEM. (D) Immunoblots depicting significant increases in tau phosphorylation at 3 other epitopes with cooling and associated quantification ($N = 3$; $n = 6$; HES1 $n = 4$, HES2 $n = 1$, IPS1 $n = 1$). Phospho-tau expression was normalized to total tau, then 37°C control. (E) Western blot quantification of PP2A-C ($N = 3$; $n = 6$; HES1 $n = 4$, HES2 $n = 1$, IPS1 $n = 1$). Note lack of effect of hypothermia, prominent expression in normal human cortex (foetal and adult positive controls) and reduced expression in Alzheimer disease affected cortex (negative control). (F) Hypothermic reduction of PP2A-C activity in hCNs (picomoles phosphate released min^{-1} μg^{-1} protein $N = 2$; $n = 8$; HES1 $n = 4$, HES2 $n = 4$). Enzyme activity presented as mean fold change relative to normothermic control + SESE, after subtraction of background phosphate; mean residual phosphate in the presence of fostriecin was 469 (SEM 27.7) picomoles μg^{-1} protein. See also Fig. S3.

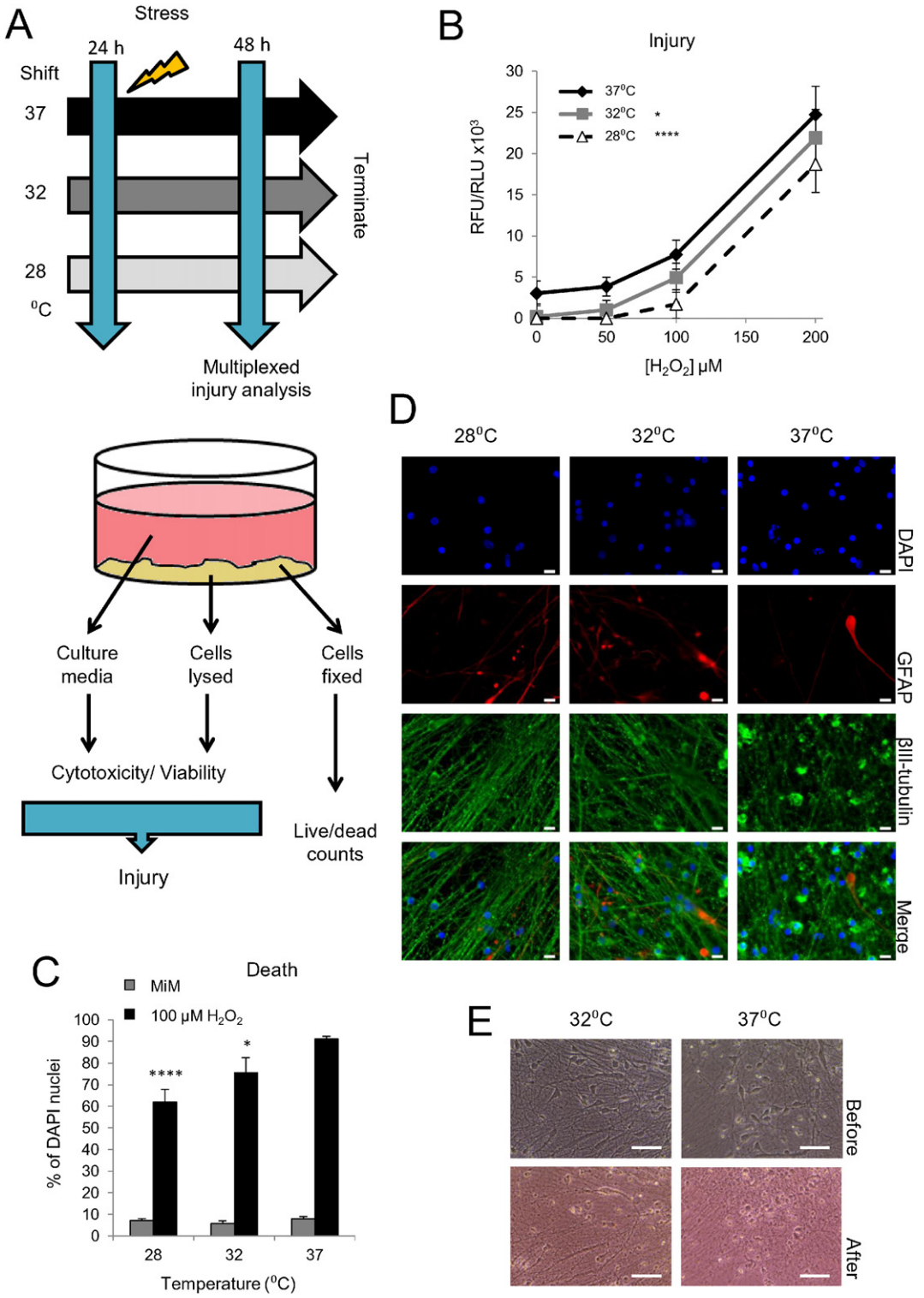

Fig. 5. Hypothermia protects hCNs from oxidative stress-mediated injury. (A) Overview of cooling and stress protocol showing temperature shift for 24 h followed by application of stressors. After 24 h of stress (total 48 h of hypothermia), multiplexed injury analysis was performed. Immunocytochemistry was used to confirm cell death by counts (100 μM H_2O_2 and 30 μM glutamate conditions only). (B) Multiplexed injury analysis with dose response curves for H_2O_2 ($N = 2$; $n = 9$; HES1 $n = 5$, HES2 $n = 4$). 200 μM H_2O_2 produced maximal injury at 37°C when compared to positive control (cell lysis with Triton-X). (C) Cell death counts ($N = 3$; $n = 8$; HES1 $n = 5$, HES2 $n = 2$, IPS1 $n = 1$). Note that incubation temperature had no effect on cell death when neurons were incubated in MiM alone. (D) Representative fluorescent micrographs of hCNs after 24 h incubation with 100 μM H_2O_2, scale bar = 10 μm. Cells were co-stained for nuclear (DAPI), neuronal (βIII-tubulin) and astrocytic (GFAP) markers. Note small number of GFAP-positive cells at each temperature, scant GFAP-positive processes and absence of neuronal processes at 37°C suggesting resistance of a few astrocytes to this concentration of H_2O_2. (E) Phase images of hCNs taken before and after incubation for 24 h with 100 μM H_2O_2 at temperatures indicated, scale bar = 20 μm. Injury data presented as point estimates (PE) ± estimated standard error (ESE) relative to normothermic control. Cell count data presented as mean + SEM. See also Figs. S4 and S5.

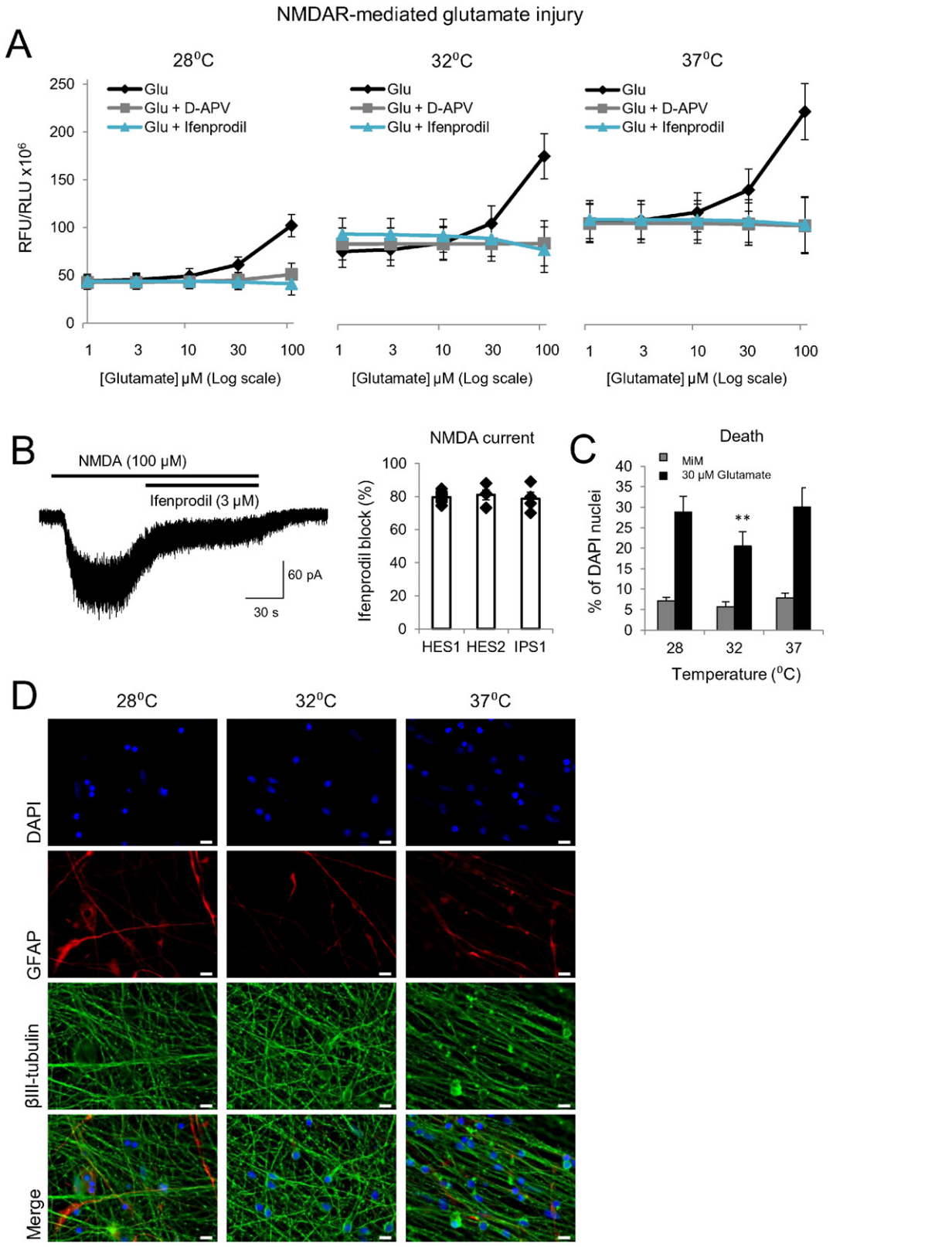

Fig. 6. Mild hypothermia protects hCNs from NMDAR-dependent glutamate excitotoxicity. (A) Dose response curves for glutamate injury in presence of specific (ifenprodil) and non-specific (D(−)-2-Amino-5-phosphonopentanoic acid, D-APV) NMDAR blockers ($N = 2$; $n = 9$; HES1 $n = 5$, HES2 $n = 4$). The 'zero treatment' control data from Fig. 5B was used to normalize responses to exogenous glutamate. Note maximal injury not achieved with 100 μM glutamate, suggesting some glutamate tolerance at baseline. Note shift of each injury curve downwards with decreasing temperature and shift upwards at 32 °C in presence of 1 μM glutamate and ifenprodil ($P = 0.001$), consistent with protective effect of low exogenous glutamate (Hardingham and Bading, 2010). Both blockers prevented the toxic effect of high glutamate, confirming that excitotoxicity was GluN2B-mediated at each temperature ($P < 0.0005$). Injury data are presented as PE ± ESE relative to normothermic control. (B) Representative current trace (left) of 5 wk-old hCNs in response to NMDA (100 μM) in presence of glycine (50 μM) at a holding potential of −74 mV. Application of 3 μM ifenprodil (a GluN2B-specific inhibitor) produces approximately 80% block of NMDA-mediated current, confirming it is largely mediated by GluN1/GluN2B-containing NMDARs. Mean % NMDA receptor block ± SEM was equivalent across all cell lines investigated (right, HES1 $n = 14$ cells from 4 independent batches, HES2 $n = 4$ cells from 1 batch, IPS1 $n = 4$ cells from 1 batch). (C) Cell death counts in response to 30 μM glutamate presented as mean + SEM ($N = 3$; $n = 8$; HES1 $n = 5$, HES2 $n = 2$, IPS1 $n = 1$) and confirmed a 31.8% reduction in cell death at 32 °C ($P = 0.001$). (D) Representative images of hCNs after 24 h incubation with 30 μM glutamate scale bar = 10 μm. See also Figs. S4 and S5.

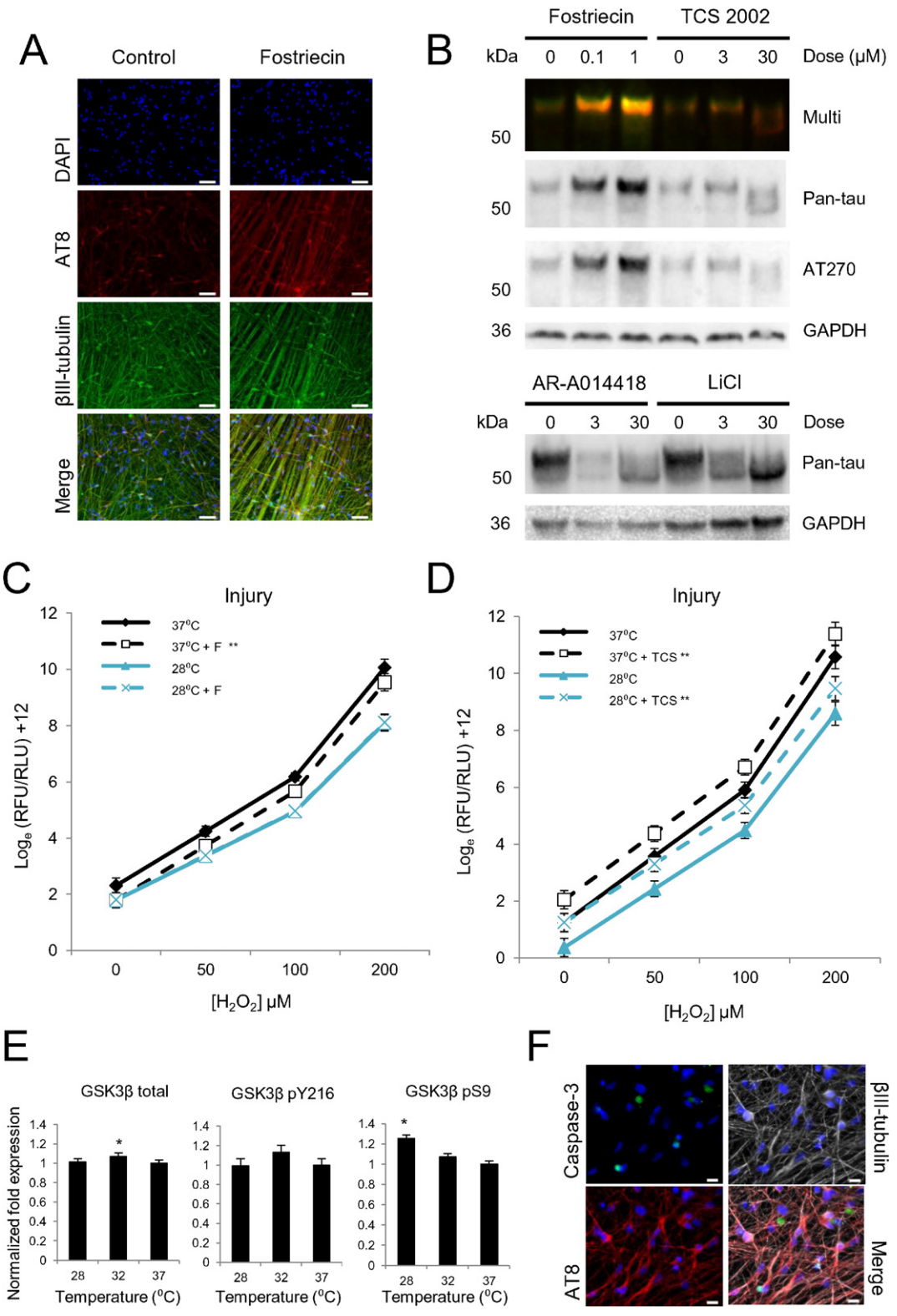

Fig. 7. Hypothermic neuroprotection is mediated by PP2A inhibition. (A) Fostriecin treatment of normothermic hCNs increases tau phosphorylation as shown by enhanced AT8 immunolabelling (100 nM fostriecin, scale bar = 50 μm) and (B) concentration-dependent increase in AT270 and pan-tau signals on Western blot with decreased electrophoretic mobility. Tau kinase (GSK3β) inhibitor TCS 2002 decreases tau phosphorylation in a concentration-dependent manner and at high concentrations resolves the protein into its dephosphorylated isoforms of lower molecular weight (upper blot). Commonly used GSK3 inhibitors have an effect on normothermic tau (lower blot), comparable to that of TCS 2002 (Saitoh et al., 2009). AR-014418 concentrations are in μM, those for LiCl are in mM. The pan-tau antibody recognises phosphorylated and non-phosphorylated tau, GAPDH = loading control. (C) Fostriecin reduces H_2O_2-mediated injury ($N = 3$; $n = 6$; HES1 $n = 3$, HES2 $n = 1$, IPS1 $n = 1$) but has no effect on injury when hCNs are incubated at 28°C. (D) TCS 2002 increases H_2O_2-mediated injury at 37°C and 28°C ($N = 3$; $n = 4$; HES1 $n = 1$, HES2 $n = 1$, IPS1 $n = 2$). Note that y-axis has been logged for both (C) and (D). (E) Quantification by Western blot of total, activated (phosphorylated at Y216) and deactivated (phosphorylated at S9) GSK3β expression at 3 temperatures. For total and pS9, $N = 3$; $n = 4$; HES1, n = 2; HES2, $n = 1$, IPS1, $n = 1$; for pY216, $N = 3$; $n = 6$; HES1, n = 4; HES2, $n = 1$, IPS1, $n = 1$. Total GSK3β expression was normalized to GAPDH, phosphorylated GSK3β was normalized to total GSK3β. GSK3β phosphorylates tau and is recognised as an apoptosis inducer (Meares et al., 2011). Note increase in the deactivated form at 28 °C ($P = 0.018$). (F) Fluorescent micrographs of hypothermic hCNs showing mutually exclusive staining of phospho-tau (AT8) and apoptotic marker activated caspase-3. Cells were co-stained for DAPI and neuronal marker βIII-tubulin, scale bar = 10 μm.

Role of Funding Sources

Funding sources did not have any involvement in the study design; the collection, analysis and interpretation of data; writing of the report; or the decision to submit the article for publication. The authors declare no conflicts of interest.

Acknowledgements

We thank the MRC Edinburgh Brain & Tissue Bank, N Khan and D Hay (both MRC Centre for Regenerative Medicine), S Mitchell (Electron Microscopy Facility), J Qiu (Centre for Integrative Physiology) T Wishart (Roslin Institute), Z Krejciova (formerly NCJD Unit) past and present members of the Chandran Lab at the University of Edinburgh and P Davies (Albert Einstein College of Medicine of Yeshiva University). Funding was provided by a Wellcome Trust Integrated Training Fellowship for Veterinarians (096409/Z/11/Z to N.M.R), an Anne Rowling Senior Clinical Research Fellowship (to P.C.), a Wellcome Trust and Scottish Medicine and Therapeutics Clinical Research Training Fellowship (to S.B.), an Anne Rowling Fellowship and Wellcome Trust Intermediate Clinical Fellowship (101149/Z/13/Z to R.P.) a Wellcome Trust Grant (092742/Z/10/Z to D.J.A.W, S.C. and G.E.H), a Medical Research Council Senior Nonclinical Research Fellowship (G0902044 to G.E.H), and the Euan MacDonald Centre (to S.C.)

Appendix A. Supplemental information

Supplemental information to this article includes 5 supplemental figures, supplemental materials and methods, and supplemental references and can be found online at http://dx.doi.org/10.1016/j.ebiom.2015.12.010.

References

Aarts, E., Verhage, M., Veenvliet, J.V., Dolan, C.V., van der Sluis, S., 2014. A solution to dependency: using multilevel analysis to accommodate nested data. Nat. Neurosci. 17, 491–496.

Andrews, P.J.D., Sinclair, L., Rodriguez, A., Harris, B.A., Battison, C.G., Rhodes, J.K.J., Murray, G.D., Eurotherm3235 Trial Collaborators, 2015. Hypothermia for intracranial hypertension after traumatic brain injury. N. Engl. J. Med. (Epub ahead of print).

Antonic, A., Dottori, M., Leung, J., Sidon, K., Batchelor, P.E., Wilson, W., Macleod, M.R., Howells, D.W., 2014. Hypothermia protects human neurons. Int. J. Stroke 9, 544–552.

Arendt, T., Stieler, J., Strijkstra, A.M., Hut, R.A., Rüdiger, J., Van der Zee, E.A., Harkany, T., Holzer, M., Härtig, W., 2003. Reversible paired helical filament-like phosphorylation of tau is an adaptive process associated with neuronal plasticity in hibernating animals. J. Neurosci. 23, 6972–6981.

Bilican, B., Livesey, M.R., Haghi, G., Qiu, J., Burr, K., Siller, R., Hardingham, G.E., Wyliie, D.J., Chandran, S., 2014. Physiological normoxia and absence of EGF is required for the long-term propagation of anterior neural precursors from human pluripotent cells. PLoS One 9, e85932.

Bretteville, A., Marcouiller, F., Julien, C., El Khoury, N.B., Petry, F.R., Poitras, I., Mouqinot, D., Levesque, G., Hebert, S.S., Planel, E., 2012. Hypothermia-induced hyperphosphorylation: a new model to study tau kinase inhibitors. Sci. Rep. 2, 480.

Brion, J.-P., Smith, C., Couck, A.-M., Gallo, J.-M., Anderton, B.H., 1993. Developmental changes in tau phosphorylation: fetal τ is transiently phosphorylated in a manner similar to paired helical filament-τ characteristic of Alzheimer's disease. J. Neurochem. 61, 2071–2080.

Busto, R., Globus, M.Y., Dietrich, W.D., Martinez, E., Valdés, I., Ginsberg, M.D., 1989. Effect of mild hypothermia on ischemia-induced release of neurotransmitters and free fatty acids in rat brain. Stroke 20, 904–910.

Chip, S., Zelmer, A., Ogunshola, O.O., Felderhoff-Mueser, U., Nitsch, C., Bührer, C., Wellmann, S., 2011. The RNA binding protein RBM3 is involved in hypothermia induced neuroprotection. Neurobiol. Dis. 43, 388–396.

Dietrich, W.D., Atkins, C.M., Bramlett, H.M., 2009. Protection in animal models of brain and spinal cord injury with mild to moderate hypothermia. J. Neurotrauma 26, 301–312.

Espuny-Camacho, I., Michelsen, K.A., Gall, D., Linaro, D., Hasche, A., Bonnefont, J., Bali, C., Orduz, D., Bilheu, A., Herpoel, A., et al., 2013. Pyramidal neurons derived from human pluripotent stem cells integrate efficiently into mouse brain circuits in vivo. Neuron 77, 440–456.

Goedert, M., Jakes, R., 1990. Expression of separate isoforms of human tau protein: correlation with the tau pattern in brain and effects on tubulin polymerization. EMBO J. 9, 4225–4230.

Goedert, M., Spillantini, M.G., Jakes, R., Rutherford, D., Crowther, R.A., 1989a. Multiple isoforms of human microtubule-associated protein tau: sequences and localization in neurofibrillary tangles of Alzheimer's disease. Neuron 3, 519–526.

Goedert, M., Spillantini, M.G., Potier, M.C., Ulrich, J., Crowther, R.A., 1989b. Cloning and sequencing of the cdna encoding an isoform of microtubule-associated protein tau containing four tandem repeats: differential expression of tau protein MRNAs in human brain. EMBO J. 8, 393–399.

Gong, C.X., Lidsky, T., Wegiel, J., Zuck, L., Grundke-Iqbal, I., Iqbal, K., 2000. Phosphorylation of microtubule-associated protein tau is regulated by protein phosphatase 2A in mammalian brain. Implications for neurofibrillary degeneration in Alzheimer's disease. J. Biol. Chem. 275, 5535–5544.

Gupta, K., Hardingham, G.E., Chandran, S., 2013. NMDA receptor-dependent glutamate excitotoxicity in human embryonic stem cell-derived neurons. Neurosci. Lett. 543, 95–100.

Hardingham, G.E., Bading, H., 2010. Synaptic versus extrasynaptic NMDA receptor signalling: implications for neurodegenerative disorders. Nat. Rev. Neurosci. 11, 682–696.

Iqbal, K., Liu, F., Gong, C.X., Alonso Adel, C., Grundke-Iqbal, I., 2009. Mechanisms of tau-induced neurodegeneration. Acta Neuropathol. 118, 53–69.

Jacobs, S.E., Berg, M., Hunt, R., Tarno-Mordi, W.O., Inder, T.E., Davis, P.G., 2013. Cooling for newborns with hypoxic ischaemic encephalopathy. Cochrane Database Syst. Rev. 1, CD003311.

James, O.T., Livesey, M.R., Qiu, J., Dando, O., Bilican, B., Haghi, G., Rajan, R., Burr, K., Hardingham, G.E., Chandran, S., Kind, P.C., Wyllie, D.J., 2014. Ionotropic GABA and glycine receptor subunit composition in human pluripotent stem cell-derived cortical neurones. J. Physiol. 592, 4353–4363.

Janke, C., Beck, M., Stahl, T., Holzer, M., Brauer, K., Bigl, V., Arendt, T., 1999. phylogenetic diversity of the expression of the microtubule associated protein tau: implications for neurodegenerative disorders. Brain Res. Mol. Brain Res. 68, 119–128.

Li, H.-L., Wang, H.H., Liu, S.J., Deng, Y.Q., Zhang, Y.J., Tian, Q., Wang, X.C., Chen, X.Q., Yang, Y., Zhang, J.Y., 2007. Phosphorylation of tau antagonizes apoptosis by stabilizing β-catenin, a mechanism involved in Alzheimer's neurodegeneration. Proc. Natl. Acad. Sci. U. S. A. 104, 3591–3596.

Liu, X.A., Song, J., Jiang, Q., Wang, Q., Tian, Q., Wang, J.Z., 2012. Expression of the hyperphosphorylated tau attenuates ER stress-induced apoptosis with upregulation of unfolded protein response. Apoptosis 17, 1039–1049.

Livesey, M.R., Bilican, B., Qiu, J., Rzechorzek, N.M., Haghi, G., Burr, K., Hardingham, G.E., Chandran, S., Wyllie, D.J., 2014. Maturation of AMPAR composition and the $GABA_AR$ reversal potential in hPSC-derived cortical neurons. J. Neurosci. 34, 4070–4075.

Lleonart, M.E., 2010. A new generation of proto-oncogenes: cold-inducible RNA binding proteins. Biochim. Biophys. Acta 1805, 43–52.

Lopresti, P., Szuchet, S., Papasozoomenos, S.C., Zinkowski, R.P., Binder, L.I., 1995. Functional implications for the microtubule-associated protein tau: localization in oligodendrocytes. Proc. Natl. Acad. Sci. U. S. A. 92, 10369–10373.

Matsuo, E.S., Shin, R.W., Billingsley, M.L., Van deVoorde, A., O'Connor, M., Trojanowski, J.Q., Lee, V.M., 1994. Biopsy-derived adult human brain tau is phosphorylated at many of the same sites as Alzheimer's disease paired helical filament tau. Neuron 13, 989–1002.

Mawal-Dewan, M., Henley, J., Ven de Voorde, A., Trojanowski, J.Q., Lee, V.M., 1994. The phosphorylation state of tau in the developing rat brain is regulated by phosphoprotein phosphatases. J. Biol. Chem. 269, 30981–30987.

Meares, G.P., Mines, M.A., Beurel, E., Eom, T.Y., Song, L., Zmijewska, A.A., Jope, R.S., 2011. Glycogen synthase kinase-3 regulates endoplasmic reticulum (ER) stress-induced CHOP expression in neuronal cells. Exp. Cell Res. 317, 1621–1628.

Mondragon-Rodriguez, S., Trillaud-Doppia, E., Dudilot, A., Bourgeois, C., Lauzon, M., Leclerc, N., Boehm, J., 2012. Interaction of endogenous tau with synaptic proteins is regulated by NMDA-receptor dependent tau phosphorylation. J. Biol. Chem. 287, 32040–32053.

Papadia, S., Soriano, F.X., Léveillé, F., Martel, M.A., Dakin, K.A., Hansen, H.H., Kaindl, A., Sifringer, M., Fowler, J., Stefovska, V., et al., 2008. Synaptic NMDA receptor activity boosts intrinsic antioxidant defences. Nat. Neurosci. 11, 476–487.

Peretti, D., Bastide, A., Radford, H., Verity, N., Molloy, C., Martin, M.G., Moreno, J.A., Steinert, J.R., Smith, T., Dinsdale, D., et al., 2015. RBM3 mediates structural plasticity and protective effects of cooling in neurodegeneration. Nature 518, 236–239.

Planel, E., Miyasaka, T., Launey, T., Chui, D.H., Tanemura, K., Sato, S., Murayama, O., Ishiquro, K., Tatebayashi, Y., Takashima, A., 2004. Alterations in glucose metabolism induce hypothermia leading to tau hyperphosphorylation through differential inhibition of kinase and phosphatase activities: implications for Alzheimer's disease. J. Neurosci. 24, 2401–2411.

Planel, E., Richter, K.E., Nolan, C.E., Finley, J.E., Liu, L., Wen, Y., Krishnamurthy, P., Herman, M., Wang, L., Schachter, J.B., et al., 2007. Anesthesia leads to tau hyperphosphorylation through inhibition of phosphatase activity by hypothermia. J. Neurosci. 27, 3090–3097.

Planel, E., Bretteville, A., Liu, L., Virag, L., Du, A.L., Yu, W.H., Dickson, D.W., Whittington, R.A., Duff, K.E., 2009. Acceleration and persistence of neurofibrillary pathology in a mouse model of tauopathy following anesthesia. FASEB J. 23, 2595–2604.

Rzechorzek, N.M., Connick, P., Patani, R., Selvaraj, B.T., Chandran, S., 2015. Hypothermic preconditioning of human cortical neurons requires proteostatic priming. EBioMedicine 2, 528–535.

Saitoh, M., Kunitomo, J., Kimura, E., Iwashita, H., Uno, Y., Onishi, T., Uchiyama, N., Kawamoto, T., Tanaka, T., Mol, C.D., et al., 2009. 2-{3-[4-(Alkylsulfinyl)phenyl]-1-benzofuran-5-yl}-5-methyl-1,3,4-oxadiazole derivatives as novel inhibitors of glycogen synthase kinase-3β with good brain permeability. J. Med. Chem. 52, 6270–6286.

Spillantini, M.G., Goedert, M., 2013. Tau pathology and neurodegeneration. Lancet Neurol. 12, 609–622.

Sposito, T., Preza, E., Mahoney, C.J., Seto-Salvia, N., Ryan, N.S., Morris, H.R., Arber, C., Devine, M.J., Houlden, H., Warner, T.T., et al., 2015. Developmental regulation of tau splicing in stem cell derived neurons from frontotemporal dementia patients with 10 + 16 splice-site mutation in MAPT. Hum. Mol. Genet. 24, 5260–5269.

Stieler, J.T., Bullmann, T., Kohl, F., Toien, O., Brückner, M.K., Härtig, W., Barnes, B.M., Arendt, T., 2011. The physiological link between metabolic rate depression and tau phosphorylation in mammalian hibernation. PLoS One 6, e14530.

Trojanowski, J.Q., Lee, V.M., 1995. Phosphorylation of paired helical filament tau in Alzheimer's disease: focusing on phosphatases. FASEB J. 9, 1570–1576.

Walsh, A.H., Cheng, A., Honkanen, R.E., 1997. Fostriecin, an antitumor antibiotic with inhibitory activity against serine/threonine protein phosphatases types 1 (PP1) and 2A (PP2A) is highly selective for PP2A. FEBS Lett. 416, 230–234.

Yenari, M.A., Han, H.S., 2012. Neuroprotective mechanisms of hypothermia in brain ischaemia. Nat. Rev. Neurosci. 13, 267–278.

Yu, Y., Run, X., Liang, Z., Li, Y., Liu, F., Liu, Y., Iqbl, K., Grundke-Iqbal, I., Gong, C.X., 2009. Developmental regulation of tau phosphorylation, tau kinases, and tau phosphatases. J. Neurochem. 108, 1480–1494.

Zell, S.C., Kurtz, K.J., 1985. Severe exposure hypothermia: a resuscitation protocol. Ann. Emerg. Med. 14, 339–345.

Zhu, X., Zelmer, A., Kapfhammer, J.P., Wellmann, S., 2015. Cold-inducible RMB3 inhibits PERK phosphorylation through cooperation with NF90 to protect cells from endoplasmic reticulum stress. FASEB J. (Epub ahead of print).